



Enhanced fouling resistance of surface-modified alumina membranes by controlling humic acid and negatively charged-organosilane concentrations

Jongman Lee*, Jang-Hoon Ha, In-Hyuck Song

Powder & Ceramics Division, Korea Institute of Materials Science (KIMS), 797 Changwondaero, Seongsangu, Changwon 642-831, Korea, Tel. +82 55 280 3292, Fax +82 55 280 3289, email: jmlee@kims.re.kr (J. Lee), hjhoon@kims.re.kr (J.-H. Ha), sih1654@kims.re.kr (I.-H. Song)

Received 14 March 2017; Accepted 31 August 2017

ABSTRACT

Surface modification of membranes is effective means to not only alleviate membrane fouling, but also realize sustainable membrane performance. Our research work focuses on studying the effect of organosilane grafting on the antifouling properties for water purification. It could therefore reveal the efficiency of negatively charged membranes to retard humic acid deposition and deal with harsher wastewater conditions. Membrane fouling became more severe with increasing concentrations of humic acid. However, the organosilane-grafted membranes with negative charges could successfully reduce flux decline and membrane fouling. Fouling resistance was improved in the presence of higher organosilane concentrations.

Keywords: Ceramic membrane; Surface modification; Organosilane; Antifouling; Humic acid

1. Introduction

Membrane technology for water separation and/or purification has been widely developed toward commercial application [1]. Membranes manufactured using polymers and ceramics have drawn much interest in the past decades because they are expected to realize controlled and sustainable water separation and/or purification processes [2]. To date, though a majority of the market share has been overwhelmed by polymeric membranes, ceramic membranes are generating increasingly widespread interest for usage in various applications such as wastewater treatment [3], oil–water separation [4], food industry [5], and gas separation [6]. Ceramic membranes offer numerous advantages over polymeric membranes owing to their intrinsic attributes such as relatively narrow pore size distributions and higher porosity, excellent mechanical, chemical, and thermal stability, and good hydrophilicity [7,8]. The differences in the fouling behaviors of polymeric and ceramic microfiltration membranes were recently investigated by Hofs et al. [9]. Four ceramic membranes

(Al₂O₃, ZrO₂, TiO₂, and SiC) and a polymeric membrane (polyethesulfone–polyvinylpyrrolidone) were examined, and increases in the transmembrane pressure (TMP), as a result of membrane fouling by direct filtration with surface water, were measured at a constant flux. The polymeric membrane exhibited the highest level of reversible and irreversible fouling among all tested membranes. It is widely accepted that the substantial increase in TMP exhibited by polymeric membranes is a result of not only the membrane structure (pore size and porosity), but also the isoelectric point of the foulant, hydrophilicity, and surface roughness of the membrane [10–12].

However, one of the most critical issues in the development of effective membrane processes for water treatment is membrane fouling (particularly irreversible fouling) during filtration performance. Membrane fouling results in abrupt flux decline and higher maintenance and operating costs, and limits application of the membrane technology [13]. Thus, mitigating the adsorption (or deposition) of foulants on the membrane surface is essential to developing ceramic membranes with superior fouling resistance. Numerous surface modification techniques have been reported for polymeric membranes [14]. In contrast, the surface modification of ceramic membranes has received

*Corresponding author.

less attention owing to the limited modification methods available to date.

In a previous comprehensive report, the effect of surface charges on membrane fouling resistance using humic acid as a model foulant (isoelectric point of 4.7) was examined [15]. Three organosilanes presenting neutral, positive, and negative charges were grafted onto alumina membranes through a simple silanization process. The negatively charged membranes generated higher flux patterns than the pristine alumina, positively charged, and neutral membranes. This result suggested that these negatively charged membranes would likely exhibit optimal flux behaviors such as low flux decline, high flux recovery, and low membrane fouling.

In the present study, we aimed to examine in detail the effect of organosilane grafting (on alumina membranes) on the antifouling properties of the resulting membranes with respect to (1) humic acid concentration and (2) organosilane concentration. Two organosilanes presenting neutral and negative charges were selected for grafting on alumina membranes because both generated higher flux patterns than the pristine alumina and positively charged membranes. In the first set of experiments, the concentration of the humic acid solution was varied from 10, 30 to 50 mg L⁻¹ during the fouling process, while the organosilane concentration was fixed to 0.1 M for surface modification. In the second set of experiments, the concentration of the negatively charged organosilane was varied from 0.05, 0.1 to 0.3 M, while the concentration of the humic acid solution was fixed at 30 mg L⁻¹. A schematic illustration of the surface modification process is shown in Fig. 1, and the different surface modification and fouling parameters investigated are shown in Table 1.

To evaluate the antifouling properties of the membranes against humic acid (chosen as a model foulant), the normalized flux data, morphological analysis, and qualitative membrane fouling ratio were determined during the membrane fouling experiments. The physicochemical characteristics (surface morphology, pore size distribution, chemical composition) of the organosilane-grafted membranes were determined by scanning electron microscopy, mercury intrusion porosimetry, and X-ray photoelectron spectroscopy, respectively.

2. Experimental part

2.1. Preparation of the alumina membranes

To prepare the alumina membranes, α -alumina powder with a mean particle size of 4.8 μm was purchased from Sumitomo Chemical Co. Ltd. (AM-210, Japan) and used without further treatment. Using polyethylene glycol (Sigma-Aldrich, USA) as a binder, the powder was molded into a circle and dry-pressed under a pressure of 15–20 MPa. The samples were then sintered in a furnace at a heating rate of 5°C min⁻¹ to 1600°C for 1 h. The final measured dimensions of the sintered alumina membranes were 34 mm \times 2.7 mm (diameter \times thickness).

The physico-chemical properties of alumina membranes were characterized with respect to surface morphology (Figs. 3, 5, 8), pore size distribution (Fig. 5), and zeta potential. According to our previous work [15], the isoelectric

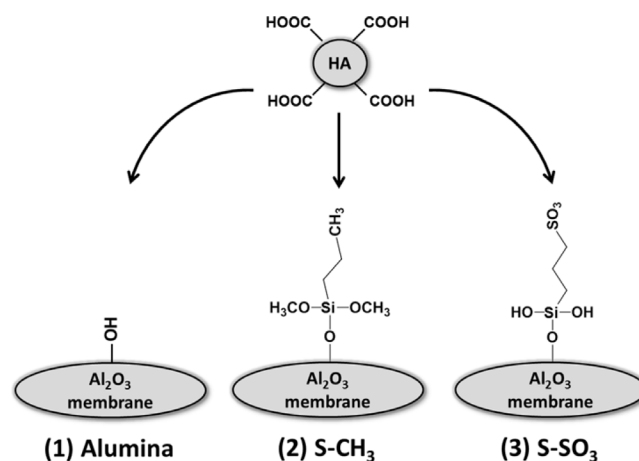


Fig. 1. Schematic diagram of the surface modification process used to prepare the organosilane-grafted alumina membranes and their interactions with negatively charged humic acid (HA).

Table 1
Experimental design adopted in the present work

(1) Effect of humic acid concentration on membrane fouling	
Membrane	Al ₂ O ₃ ; 0.1 M S-CH ₃ ; 0.1 M S-SO ₃
Humic acid solution	10, 30, and 50 mgL ⁻¹
(2) Effect of organosilane concentration (S-SO ₃) on membrane fouling	
Membrane	Al ₂ O ₃ ; 0.05 to 0.3 M S-SO ₃
Humic acid solution	30 mgL ⁻¹

points (IEP) were presented: the pristine alumina for 8.8, neutral charge membrane (S-CH₃) for 5.0, and negatively charged membrane (S-SO₃) for 3.2. At pH 6.5, strong positive charge would be shown to the pristine alumina membrane. However, strong and weak negative charges would be given to the negatively charged membrane (S-SO₃) and the neutral charge membrane (S-CH₃), respectively.

2.2. Surface modification of the alumina membranes

For the surface modification of the alumina membranes, two organosilanes were selected to introduce different surface charge properties (neutral and negative charges) on the alumina membranes. The selection of the organosilanes was based on our previous study, which revealed the relatively higher fouling resistance of negatively charged and neutral membranes over that of positively charged membranes [15].

Trimethoxy(propyl)silane (Sigma-Aldrich, USA) containing a methyl (-CH₃) group was grafted to provide a neutral charge on the resulting membrane surface. Conversely, 3-(trihydroxysilyl)-1-propanesulfonic acid (ABCR GmbH, Germany) containing a sulfonic (-SO₃) group was grafted to provide negative charges on the membrane surface.

Typically, prior to surface grafting, the alumina membranes were placed in a Petri dish and cleaned with ethanol. Individual organosilane solutions were prepared with a concentration of 0.1 M using anhydrous ethanol and added to the alumina membranes. Grafting was allowed to pro-

ceed for 5 h at 25°C under gentle shaking. Upon completion of the reaction, the organosilane solution was decanted and replaced with fresh ethanol to thoroughly rinse the alumina membranes. The surface-modified membranes were then dried at 50°C for 12 h. Consequently, the alumina membranes were chemically grafted with organosilanes possessing methyl and sulfonic groups on their surface, and the membranes were denoted as S-CH₃ and S-SO₃, respectively. To investigate the effect of organosilane concentration, the concentration of the organosilanes containing sulfonic groups was controlled from 0.05, 0.1 to 0.3 M following the same preparation procedures as above.

2.3. Characterization of the surface-modified alumina membranes

The alumina samples that underwent surface modification and membrane fouling were characterized to investigate their physicochemical properties. For the surface morphology analysis, scanning electron microscopy (SEM; JSM-6610LV, JEOL, Japan) was conducted at a magnification of 10000×. The pore size distributions of the membranes were characterized via mercury intrusion porosimetry (Autopore IV 9510, Micromeritics, USA). The chemical composition of the organosilane-grafted alumina membranes was analyzed by X-ray photoelectron spectroscopy (XPS; K-Alpha, Thermo Fisher Scientific, UK) using a monochromatic Al K α source at 1486.6 eV.

2.4. Membrane filtration set-up and fouling procedure

Membrane permeation test of the surface-modified membranes was performed using a cross-flow microfiltration system (Fig. S1) (Lab-MPT, SeptraTek Membrane System, Republic of Korea). The temperature of the feed solution was maintained at 25°C using a circulating bath (JEIO TECH, Republic of Korea). The filtration tests were then conducted at a TMP of 2.0 bar with a fluid (deionized water or humic acid solution) velocity of 2.5 L min⁻¹. Flux data were calculated based on the weight of the permeate, which was measured using an electronic mass balance (CAS, Republic of Korea).

The membrane fouling procedure consisted of seven steps according to a general membrane fouling/cleaning procedures [16]. In Step 1, the membranes were compacted using deionized (DI) water for 30 min until a stable baseline flux was attained (J_0). In Step 2, humic acid solution (Sigma-Aldrich, USA) prepared at varying concentrations (10, 30, and 50 mg L⁻¹ at pH 6.5) was introduced to induce membrane fouling for 1 h; the corresponding flux (J_{p1}) was measured. In Step 3, the fouled membranes were back-washed for 10 min using 10 mM sodium dodecyl sulfate solution (SDS; Sigma-Aldrich, USA) at pH 11. In Step 4, DI water was supplied again for 30 min to achieve a stable flux (J_1). In Step 5, humic acid solution was supplied again for a second membrane fouling process following the same method as Step 2, and the associated flux (J_{p2}) was measured. Steps 6 and 7 were subsequently undertaken to back-wash and achieve a stable flux (J_2), respectively. The overall fouling process was performed for at least thrice using the three membranes, and the mean values were used in the sub-

sequent calculations. Based on the flux data obtained, the antifouling properties i.e., flux decline ratio (%) and flux recovery ratio (%) were calculated using the following equations:

$$\text{Flux decline ratio} = \left(1 - \frac{J_{p1,p2}}{J_0} \right) \times 100\% \quad (1)$$

$$\text{Flux recovery ratio} = \left(\frac{J_{1,2}}{J_0} \right) \times 100\% \quad (2)$$

where J_0 is the DI water flux in Step 1, $J_{p1,p2}$ are the flux values of humic acid in Steps 2 and 5, respectively, and $J_{1,2}$ are the DI water flux values in Steps 4 and 7, respectively.

To quantitatively assess the antifouling performance of the membranes against humic acid, the experiments were conducted in recirculation mode. Typically, 1 L humic acid solution was supplied to the feed tank in Step 2, and the permeate was sent back to the feed tank. Then, an aliquot (10 mL) of the humic acid solution in the feed tank was collected every 10 min, and the concentration of humic acid was determined by UV-visible spectroscopy at 254 nm (Cary 5000, Agilent Technologies, USA). The membrane fouling ratio (%) was calculated using the following equation:

$$\text{Membrane fouling ratio} = \left(1 - \frac{C_p}{C_0} \right) \times 100\% \quad (3)$$

where C_0 is the initial concentration of humic acid and C_p is the concentration of humic acid measured from Step 2.

3. Results and discussion

3.1. Effect of humic acid concentration on membrane fouling behavior

In this section, the effect of humic acid concentration on the fouling behavior of the surface-modified membranes is discussed. The direct influence of humic acid concentration on the normalized flux patterns is illustrated in Fig. 2. A photograph of the different humic acid solutions examined (10, 30, and 50 mg L⁻¹) is displayed in Fig. 2d. As observed from Fig. 2a–c, the flux of the pristine alumina membrane had the tendency to decline rapidly during the first fouling cycle. The extent of rapid flux decline increased with increasing humic acid concentrations. At 10 mg L⁻¹ humic acid, the neutrally charged (S-CH₃) membranes showed the second-highest flux during the first fouling step, and during the second fouling step, the flux level of the S-CH₃ membrane was comparable with that of the negatively charged (S-SO₃) membranes. However, the extent of this fouling resistance decreased considerably at the higher humic acid concentrations (30 and 50 mg L⁻¹) throughout the entire fouling process. This result indicated that the S-CH₃ membranes were not effective in maintaining antifouling properties at high concentrations of humic acid. In contrast, among all the membranes, the S-SO₃ membranes showed the best performance (highest flux) throughout the entire fouling process and at all humic acid concentrations studied. It could thus be concluded that membrane

fouling was influenced by the foulant concentration—a more severe flux decline was obtained at higher concentrations of humic acid. However, despite the high foulant concentration, the S-SO₃ membranes could maintain high fluxes throughout the entire membrane operation and thus retard significant flux reduction to some extent because of the electrostatic repulsion between the negatively charged membrane and humic acid. Humic acid has an isoelectric point of 4.7. Thus, under the fouling conditions studied (pH 6.5), humic acid bears a negative surface charge.

As coincided with our results, it is generally acceptable that the flux decline (or membrane fouling) becomes more severe with increasing concentrations of humic acid (or foulants) [17,18]. For example, the effect of bulk concentration of humic acid on the flux was studied using polyethersulfone microfiltration membranes with a pore size of 0.16 μm [18]. The flux pattern decreased gradually with increasing humic acid concentrations from 2 to 30 mg L⁻¹. Ceramic capillary membranes with a larger pore size of 1.9 μm also suffered from a significant flux decline after only 5 min of filtration—the flux decreased to 50% and 90% in the presence of 10 and 100 mg L⁻¹ humic acid, respectively. It can be concluded that the surface modification of ceramic membranes are highly required in order to mitigate the serious membrane fouling. In particular, the negatively charged membranes exhibited the most profound effect on retaining the high fluxes throughout the entire membrane filtration process (Fig. 2).

Using Eqs. (1) and (2) and the flux data shown in Fig. 2, the flux decline ratio and flux recovery ratio displayed by the organosilane-grafted membranes in the presence of humic acid at varying concentrations were calculated. The

results are presented in Table 2. In general, the flux decline ratio of the membranes increased with increasing humic acid concentrations. However, among all of the membranes, the S-SO₃ membranes displayed the lowest flux decline ratios at all humic acid concentrations examined during both fouling processes. Furthermore, a flux recovery ratio reached almost 100% with small variations.

Regardless of the preparation condition used for preparing the membranes, typically, the flux decreased to a greater extent during the second fouling step when compared with that during the first fouling step. This phenomenon was possibly a result of the presence of humic acid remaining after back-washing and subsequent DI water flux (Steps 3 and 4)—the hydrophobicity of humic acid would likely facilitate humic acid deposition during the second fouling process. Back-washing (Step 3) was performed for 10 min only using 10 mM SDS (pH 11). The rinsing conditions (rinsing solution and rinsing time) were not optimized, as this was not within the scope of the present study. Conversely, our main focus was to evaluate the unique effectiveness of organosilane grafting onto alumina membranes to improve membrane fouling resistance.

Beyer et al. investigated the relationship among foulant, cleaning reagent, and the mechanisms of membrane fouling and cleaning using polymeric nanofiltration membranes (pore size: 0.84 nm) [16]. The membranes fouled by humic acid were cleaned with 10 mM SDS solution (pH 11) for 30 min; the flux level could be recovered by 60%. The considerable increase in contact angle after membrane fouling (20°–65°) decreased to some extent following chemical cleaning (35°). The slightly increased degree of hydrophobicity after cleaning could possibly be attributed to the presence of residual humic acid on the membrane surface. Thus,

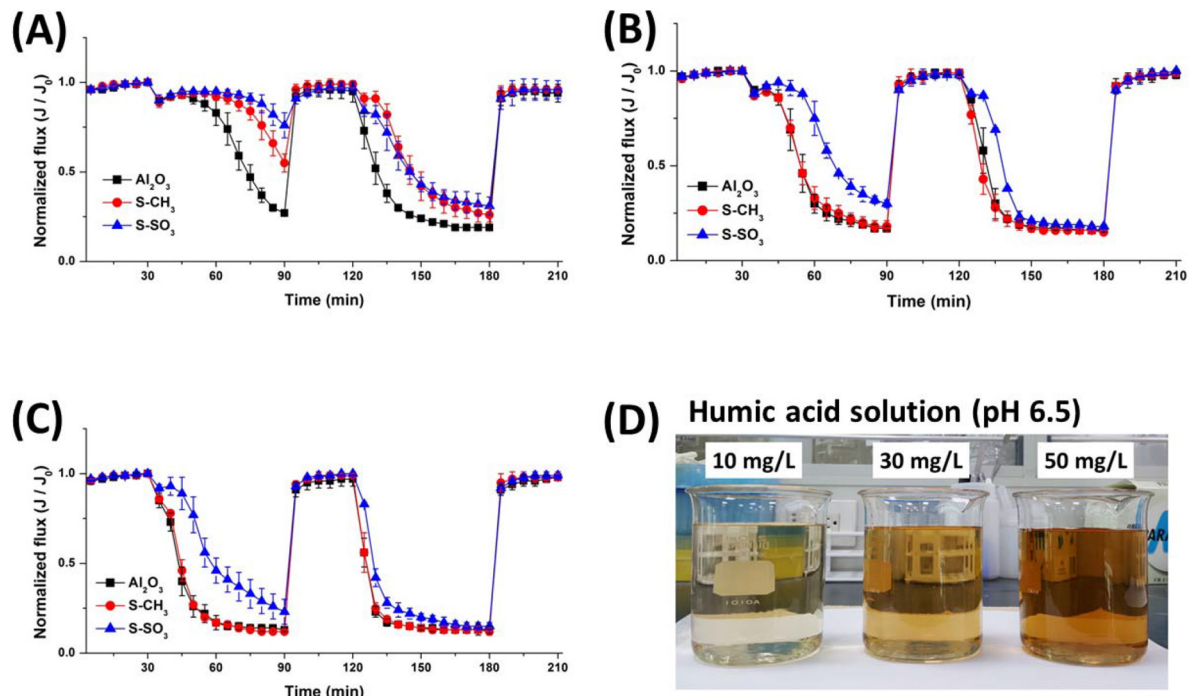


Fig. 2. Normalized flux profiles of 0.1 M organosilane-grafted membranes in the presence of humic acid at varying concentrations during membrane fouling: (A) 10, (B) 30, and (C) 50 mg L⁻¹. (D) Photographs of the humic acid solutions at varying concentrations.

Table 2

Filtration performance of the surface-modified membranes (0.1 M S-CH₃ and S-SO₃) at varying humic acid concentrations (10, 30, and 50 mg L⁻¹) during fouling (Steps 1–7)^a

10 mg/L HA	1 st fouling (Step 2)		2 nd fouling (Step 5)	
	Flux decline (%)	Flux recovery ratio (%)	Flux decline (%)	Flux recovery ratio (%)
Al ₂ O ₃	73 ± 1	95 ± 6	81 ± 1	93 ± 4
S-CH ₃	45 ± 5	99 ± 2	74 ± 4	96 ± 1
S-SO ₃	24 ± 7	97 ± 3	69 ± 5	96 ± 5
30 mg/L HA	1 st fouling (Step 2)		2 nd fouling (Step 5)	
	Flux decline (%)	Flux recovery ratio (%)	Flux decline (%)	Flux recovery ratio (%)
Al ₂ O ₃	83 ± 1	99 ± 1	85 ± 1	98 ± 2
S-CH ₃	82 ± 3	99 ± 2	85 ± 1	99 ± 2
S-SO ₃	71 ± 2	98 ± 2	83 ± 1	100 ± 1
50 mg/L HA	1 st fouling (Step 2)		2 nd fouling (Step 5)	
	Flux decline (%)	Flux recovery ratio (%)	Flux decline (%)	Flux recovery ratio (%)
Al ₂ O ₃	87 ± 1	97 ± 4	88 ± 2	98 ± 2
S-CH ₃	88 ± 1	99 ± 1	88 ± 2	99 ± 2
S-SO ₃	77 ± 7	100 ± 1	85 ± 2	99 ± 2

^aThe flux decline ratio and flux recovery ratio were calculated using Equations 1 and 2, respectively, in Section 2.4.

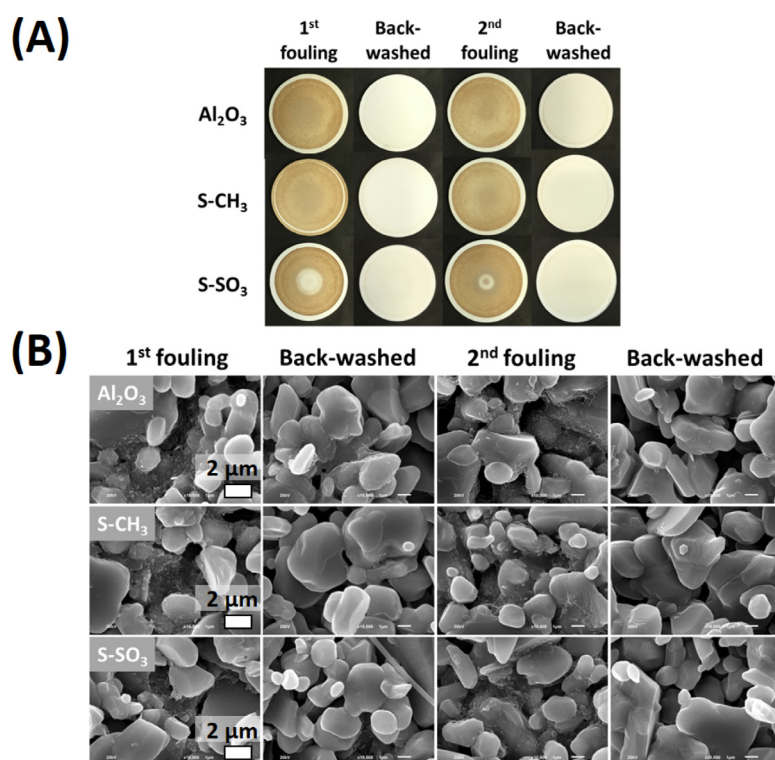


Fig. 3. (A) Photographs and (B) scanning electron microscopy (SEM) images of 0.1 M organosilane-grafted membranes during the fouling test in the presence of 30 mg L⁻¹ humic acid solution foulant. For the SEM measurement, specimens were observed at a magnification of 10,000 \times .

a fairly hydrophobic membrane surface could promote rapid flux decline, as consistent with the results in Fig. 2.

Typical photographs of the membranes fouled at 30 mg L⁻¹ humic acid and the corresponding SEM images are shown in Fig. 3a and 3b, respectively. The pristine alu-

mina and S-CH₃ membranes suffered from a high degree of fouling by humic acid (as indicated by the dark brown appearance of the membranes) in both fouling procedures (Steps 2 and 5). However, the brown coloration of the membranes lightened considerably upon backwashing (Steps 3

and 6). In contrast, the S-SO₃ membrane displayed a weaker fouling behavior than the other two samples. The photographs of the S-SO₃ membrane were consistent with the SEM analysis, which revealed the smaller deposition of humic acid on the membrane when compared with that on the other two membranes.

Thus, the above results confirm that membrane fouling is directly proportional to humic acid concentration. Though a higher degree of membrane fouling is expected with increasing humic acid concentrations, the S-SO₃ membranes, obtained via a simple sulfonation process, could afford outstanding antifouling performance at all humic acid concentrations. This superior performance was attributed to the strong electrostatic repulsion force between the negatively charged humic acid and negatively charged surface-modified membrane.

Additionally, the membrane fouling ratio of the organosilane-grafted membranes was determined, as shown in Fig. 4. As consistent with the aforementioned results, the membrane fouling ratio increased with increasing humic acid concentrations. Among all membranes, the S-SO₃ membrane displayed the weakest fouling behavior at all humic acid concentrations studied. The S-CH₃ membrane also displayed fairly strong fouling resistance, however, only at the lower humic acid concentrations (10 and 30 mg L⁻¹).

3.2. Effect of organosilane concentration on membrane fouling behavior

In this section, the effect of organosilane concentration on the membrane fouling behavior of the surface-modified membranes was examined. Organosilanes containing sulfonic (–SO₃) groups at three different concentrations (0.05, 0.1, and 0.3 M) were selected to prepare the S-SO₃ membranes. First, the influence of the grafting conditions on the membrane properties is discussed.

The pore size distributions, obtained by mercury intrusion porosimetry analysis, of the organosilane-grafted membranes are illustrated in Fig. 5. The organosilane-grafted membranes displayed smaller pore sizes (0.73–0.78 μm) when compared with the pristine alumina membrane (0.90 μm). The different organosilane-grafted membranes displayed comparable pore sizes. As consistent with our previous results [15], the pore size reduction was mainly ascribed to the newly formed organosilane layers with a thickness of ~60–85 nm. Additionally, no significant morphological changes were observed among the membranes grafted with the different concentrations of organosilane (insert of Fig. 5).

The chemical composition of the organosilane-grafted alumina membranes was determined by XPS. The survey and C1s, S2p, and Si2p XPS spectra of the membranes are shown in Fig. 6A and Fig. 6B–D, respectively. Characteristic

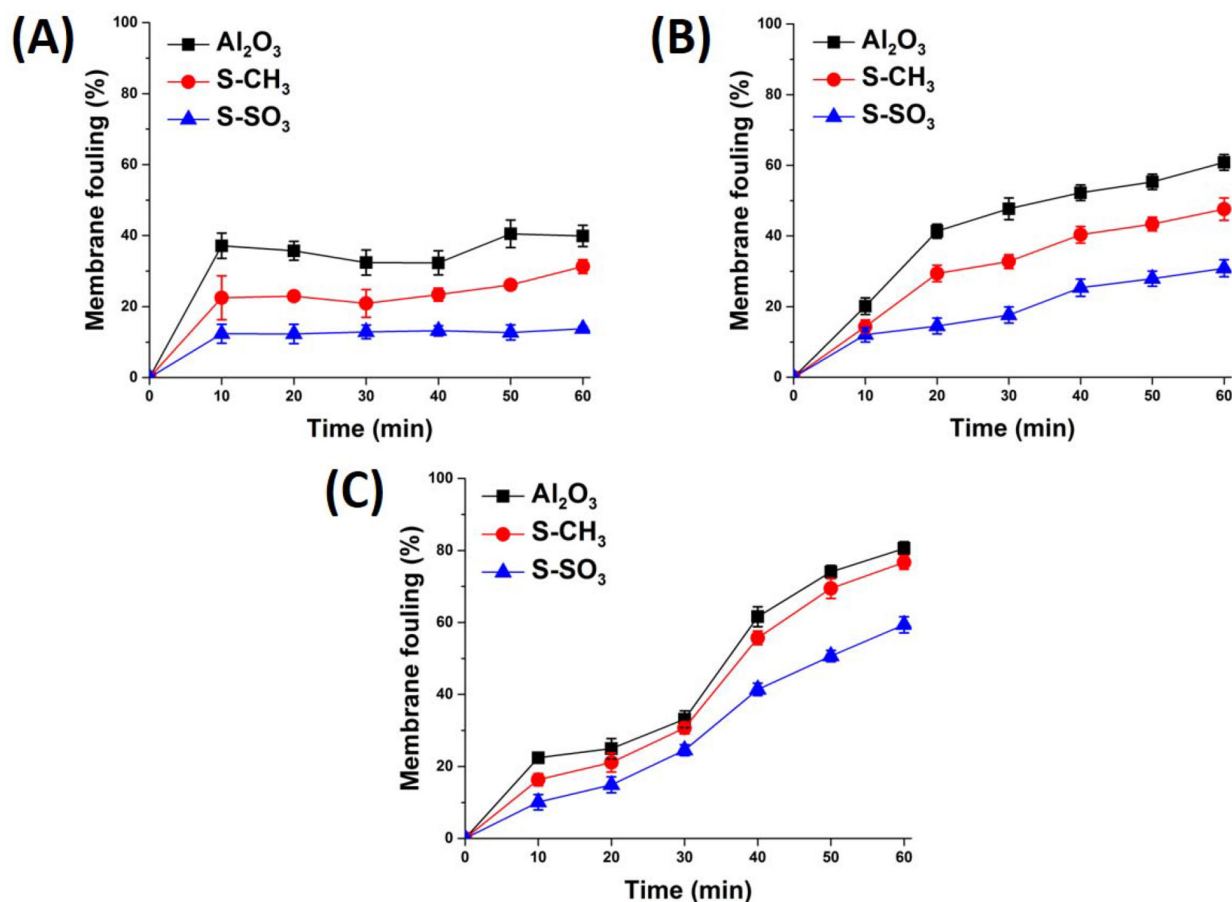


Fig. 4. Quantitative analysis of the antifouling performance of the organosilane-grafted membranes against humic acid in Step 2 performed in recirculation mode. The humic acid concentration was varied from (A) 10, (B) 30 to (C) 50 mg L⁻¹.

peaks of the organosilane-grafted membranes (S-SO₃) were observed at 285 eV (C1s), 169 eV (S2p), and 103 eV (Si2p). The intensities of the three peaks were comparable at all three organosilane concentrations. The XPS results additionally revealed that the pristine alumina membrane contained some carbon (C1s peak) and silicone (Si2p peak) contaminants, however, at negligible levels when compared with those of the other organosilane-grafted membranes [19].

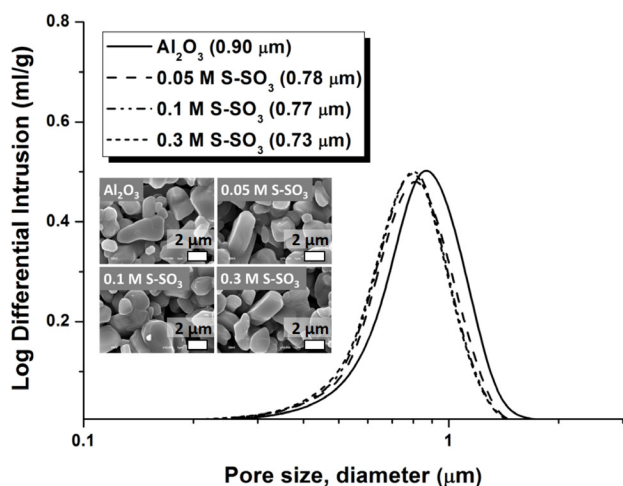


Fig. 5. Pore size distribution of the S-SO₃-modified alumina membranes prepared with different concentrations of organosilane: 0 M (pristine alumina membrane) and 0.05–0.3 M. The insets show SEM images of the corresponding membranes.

The normalized flux patterns of the S-SO₃ membranes prepared at different organosilane concentrations are presented in Fig. 7. The concentration of the humic acid solution was set at 30 mg L⁻¹. As expected, the membranes prepared at higher organosilane concentrations generated greater flux patterns; the S-SO₃ membrane prepared at an organosilane concentration of 0.3 M displayed the greatest flux level among all three S-SO₃ membranes. Hence, it could be concluded that the former S-SO₃ membrane (0.3 M organosilane) displayed the greatest fouling resistance. This

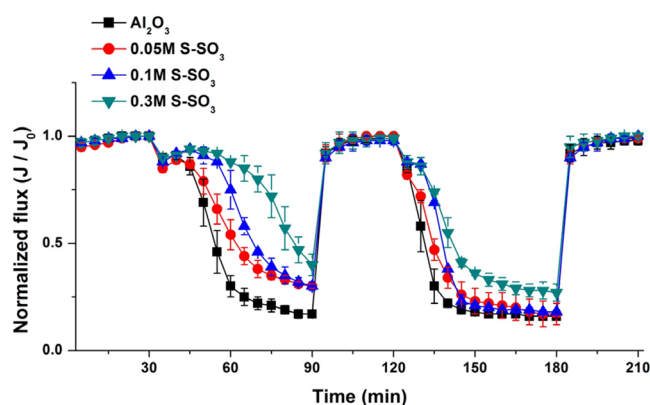


Fig. 7. Normalized flux profiles of the S-SO₃-modified membranes prepared at different concentrations (0–0.3 M) of organosilane during membrane fouling (Steps 1–7). The concentration of the humic acid solution was fixed at 30 mg L⁻¹.

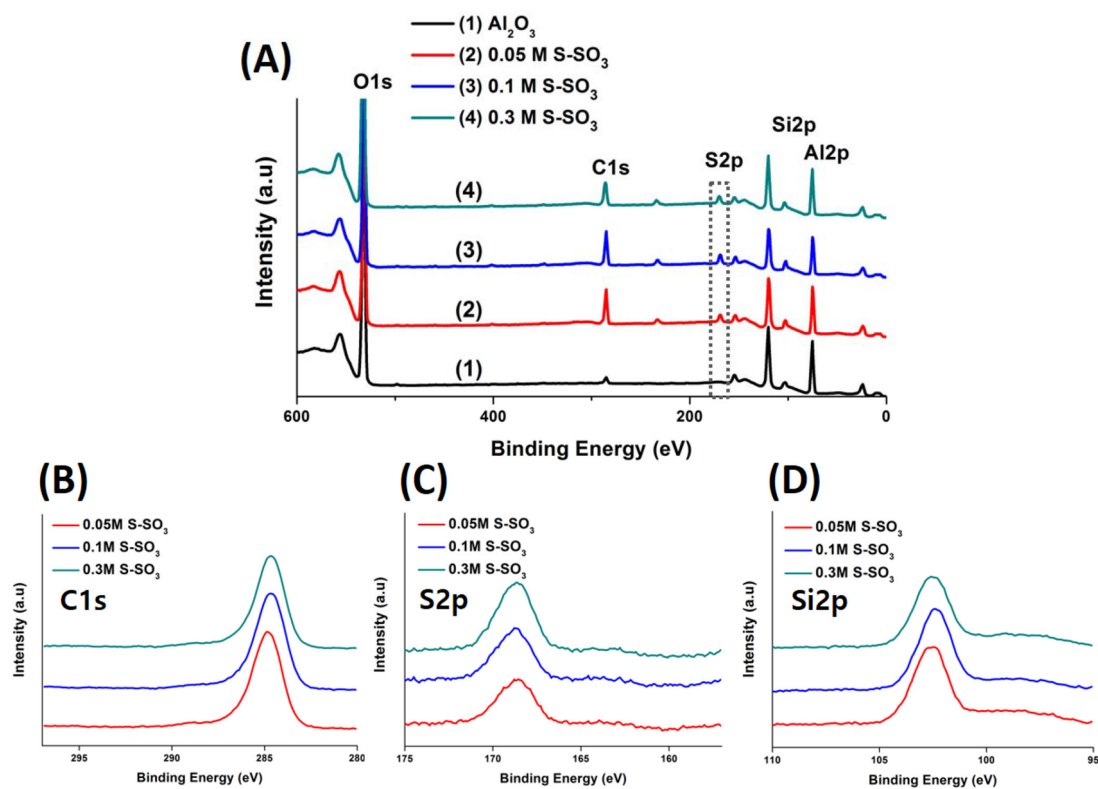


Fig. 6. (A) Full scan and (B) C1s, (C) S2p, and (D) Si2p XPS patterns of the organosilane-grafted alumina membranes prepared at different concentrations of organosilane.

result was attributed to the electrostatic repulsion force between the membrane and foulant, which became considerably stronger with increasing organosilane concentrations from 0.05 to 0.3 M.

Table 3 lists the flux decline ratio and flux recovery ratio obtained for the S-SO₃ membranes prepared at different organosilane concentrations. In general, the flux decline ratio decreased with increasing organosilane concentrations from 0.05 to 0.3 M. Furthermore, all three S-SO₃ membranes could attain a flux recovery ratio of ~100%. Thus, it could be concluded that the antifouling properties of the membranes were directly proportional to the amount of organosilanes grafted onto the membranes during surface modification.

Typical photographs of the membranes subjected to fouling and their corresponding SEM images are shown in

Fig. 8A and B, respectively. The results were consistent with those observed in Fig. 7. Specifically, as observed in Fig. 8, membrane fouling became less severe with increasing organosilane concentrations.

The membrane fouling ratio of the organosilane-grafted membranes was also determined, and the results are shown in Fig. 9. The results agreed with the aforementioned results (Figs. 7 and 8). Owing to the efficacy of organosilane (–SO₃) grafting, lower membrane fouling ratios were obtained with increasing organosilane concentrations from 0.05 to 0.3 M. Thus, higher levels of –SO₃ grafting could improve fouling resistance against humic acid.

In our previous study [15], we reported the remarkable performance of negatively charged (S-SO₃) ceramic membranes in improving antifouling properties. The neg-

Table 3

Filtration performance of the surface-modified membranes (0.05, 0.1, and 0.3 M S-SO₃) at a fixed humic acid solution concentration (30 mg L⁻¹) during fouling (Steps 1–7)^a

30 mg/L HA	1 st fouling (Step 2)		2 nd fouling (Step 5)	
	Flux decline (%)	Flux recovery ratio (%)	Flux decline (%)	Flux recovery ratio (%)
0.05 M S-SO ₃	70 ± 1	100 ± 0	83 ± 5	99 ± 1
0.1 M S-SO ₃	71 ± 2	98 ± 2	84 ± 3	100 ± 1
0.3 M S-SO ₃	61 ± 5	99 ± 1	74 ± 4	100 ± 1

^aThe flux decline ratio and flux recovery ratio were calculated using Eqns. (1) and (2), respectively, in Section 2.4.

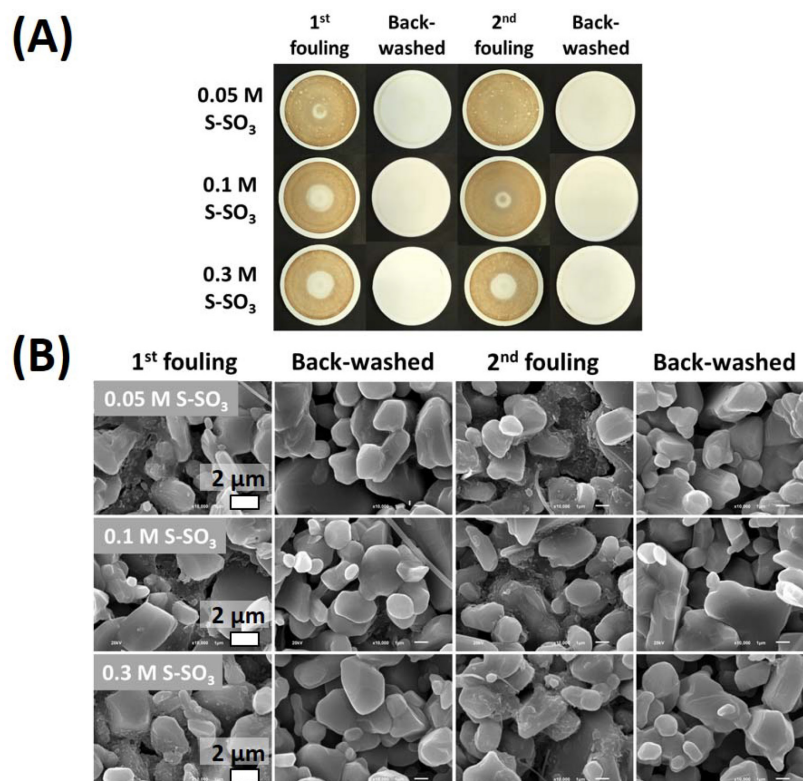


Fig. 8. (A) Photographs and (B) SEM images of negatively-charged membranes (0.05, 0.1, and 0.3 M S-SO₃) during the filtration test using 30 mg L⁻¹ humic acid solution as foulant. For the SEM measurement, specimens were observed at a magnification of 10,000 \times .

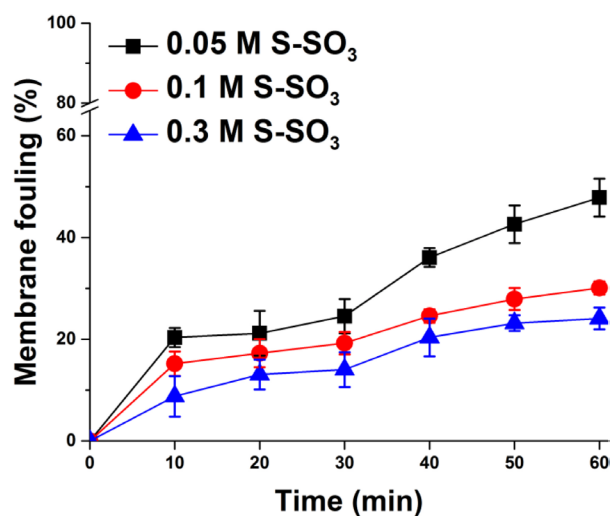


Fig. 9. Quantitative analysis of the antifouling performance of the organosilane-grafted membranes against humic acid in Step 2 performed in recirculation mode.

atively charged organosilane-functionalized membranes were prepared via a simple chemical reaction using sulfonic group-containing organosilanes. In contrast to our approach, to date, most surface modification processes have been conducted on polymeric membranes via either physical and/or chemical treatments or hybridization of organic and/or inorganic materials [20,21]. However, the development of surface modification techniques for ceramic membranes is considered to be as important, if not more valuable, owing to the increasing applications of ceramic membranes.

4. Conclusions

Currently, much attention is increasingly being devoted to studying the effect of organosilane grafting on the antifouling properties of ceramic membranes for water purification. Based on the previous paper showing the superiority of the organosilane-grafted membranes, we aimed to prove the efficacy of surface modification techniques in improving the antifouling properties of membranes subjected to harsher wastewater conditions such as the high concentrations of foulants. The performance of the organosilane-grafted ceramic membranes was explained in terms of humic acid concentration and organosilane ($-\text{SO}_3$) concentration. Membrane fouling increased with increasing humic acid concentrations. However, the negatively charged organosilane-grafted membranes successfully reduced flux decline and membrane fouling. The membrane fouling resistance improved further as the organosilane ($-\text{SO}_3$) concentration increased from 0.05 to 0.3 M.

Acknowledgements

This work was supported by the Technology Innovation Program (10053611) of the Ministry of Trade, Industry & Energy (MI, Republic of Korea).

References

- [1] W. Yang, N. Cicek, J. Ilg, State-of-the-art of membrane bioreactors: Worldwide research and commercial applications in North America, *J. Membr. Sci.*, 270 (2006) 201–211.
- [2] M.R. Wiesner, S. Chellam, The promise of membrane technology, *Environ. Sci. Technol.*, 33 (1999) 360A–366A.
- [3] S. Masmoudi, R.B. Amar, A. Larbot, H. El Feki, A.B. Salah, L. Cot, Elaboration of inorganic microfiltration membranes with hydroxyapatite applied to the treatment of wastewater from sea product industry, *J. Membr. Sci.*, 247 (2005) 1–9.
- [4] C. Yang, G. Zhang, N. Xu, J. Shi, Preparation and application in oil–water separation of $\text{ZrO}_2/\alpha\text{-Al}_2\text{O}_3$ MF membrane, *J. Membr. Sci.*, 142 (1998) 235–243.
- [5] A. Ambrosi, N. Cardozo, I. Tessaro, Membrane separation processes for the beer industry: a review and state of the art, *Food Bioprocess Tech.*, 7 (2014) 921–936.
- [6] A. Ahmad, M. Othman, N. Idrus, Synthesis and characterization of nano-composite Alumina–Titania ceramic membrane for gas separation, *J. Am. Ceram. Soc.*, 89 (2006) 3187–3193.
- [7] H. Verweij, Ceramic membranes: Morphology and transport, *J. Mater. Sci.*, 38, 4677–4695.
- [8] L. Cot, A. Ayril, J. Durand, C. Guizard, N. Hovnanian, A. Julbe, A. Larbot, Inorganic membranes and solid state sciences, *Solid State Sci.*, 2 (2000) 313–334.
- [9] B. Hofs, J. Ogier, D. Vries, E.F. Beerendonk, E.R. Cornelissen, Comparison of ceramic and polymeric membrane permeability and fouling using surface water, *Separ. Purif. Technol.*, 79 (2011) 365–374.
- [10] G.N.B. Baroña, B.J. Cha, B. Jung, Negatively charged poly(vinylidene fluoride) microfiltration membranes by sulfonation, *J. Membr. Sci.*, 290 (2007) 46–54.
- [11] H. Huang, T. Young, J.G. Jacangelo, Novel approach for the analysis of bench-scale, low pressure membrane fouling in water treatment, *J. Membr. Sci.*, 334 (2009) 1–8.
- [12] E.M. Vrijenhoek, S. Hong, M. Elimelech, Influence of membrane surface properties on initial rate of colloidal fouling of reverse osmosis and nanofiltration membranes, *J. Membr. Sci.*, 188 (2001) 115–128.
- [13] M.A. Shannon, P.W. Bohn, M. Elimelech, J.G. Georgiadis, B.J. Marinas, A.M. Mayes, Science and technology for water purification in the coming decades, *Nature*, 452 (2008) 301–310.
- [14] D. Rana, T. Matsuura, Surface modifications for antifouling membranes, *Chem. Rev.*, 110 (2010) 2448–2471.
- [15] J. Lee, J.-H. Ha, I.-H. Song, Improving the antifouling properties of ceramic membranes via chemical grafting of organosilanes, *Sep. Sci. Technol.*, 51 (2016) 2420–2428.
- [16] M. Beyer, B. Lohrengel, L.D. Nghiem, Membrane fouling and chemical cleaning in water recycling applications, *Desalination*, 250 (2010) 977–981.
- [17] M. Nyström, K. Ruohomäki, L. Kaipia, Humic acid as a fouling agent in filtration, *Desalination*, 106 (1996) 79–87.
- [18] W. Yuan, A.L. Zydney, Humic acid fouling during microfiltration, *J. Membr. Sci.*, 157 (1999) 1–12.
- [19] D. Cousens, B. Wood, J. Wang, A. Atrens, Implications of specimen preparation and of surface contamination for the measurement of the grain boundary carbon concentration of steels using x-ray microanalysis in an UHV FESEM, *Surf. Interface Anal.*, 29 (2000) 23–32.
- [20] G.-d. Kang, Y.-m. Cao, Development of antifouling reverse osmosis membranes for water treatment: A review, *Water Res.*, 46 (2012) 584–600.
- [21] X. Li, J. Huang, Y. Zhang, Y. Lv, Z. Liu, Z. Shu, Characterization and antifouling performance of negatively charged PES/mesoporous silica ultrafiltration membrane for raw water filtration, *Desalin. Water Treat.*, 57(24) (2016) 10980–10987.